PAMM · Proc. Appl. Math. Mech. **17**, 381 – 382 (2017) / **DOI** 10.1002/pamm.201710160

Oscillations of a visco-elastic belt drive

Alois Steindl[1,*]

[1] Institute for Mechanics and Mechatronics, TU Wien; Getreidemarkt 9; 1060 Wien

We investigate the loss of stability of the steady configuration of a planar visco-elastic belt drive. The belt is considered as a linearly visco-elastic slender beam with small bending stiffness, which is driven by a steadily rotating drum. Due to the presence of the small damping parameter and the small bending stiffness, the equations of motion are severly singularly perturbed. By variation of system parameters, like the driving speed, the damping coefficient, the tension force and the radius of the drums, we calculate the steady configuration and the stability limit of the belt. Our calculations show, that the viscous damping, the distributed load and the strong bending at the drums can decrease the critical driving speed significantly and lead to flutter oscillations.

1 Introduction and model setup

Drive belts are frequently used tools for power transmission and their stable behaviour is important for the proper operation of the facility. For slowly moving belts it is usually sufficient to consider the equilibrium states, but if the belt speed approaches the wave speed in the belt, the influence of the drive motion has to be taken into account.

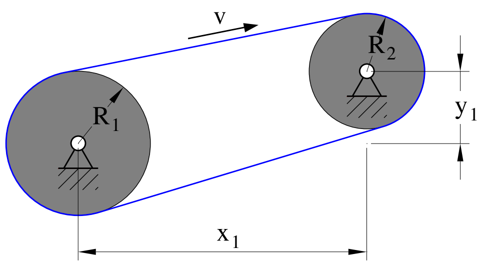

Fig. 1: Mechanical model of the belt drive moving with velocity v

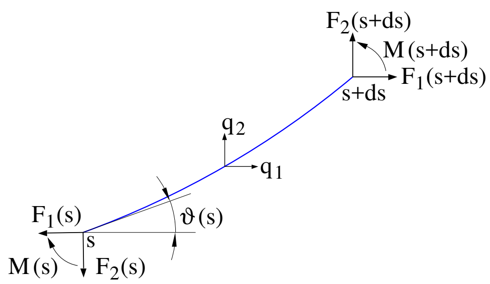

Fig. 2: Cross-sectional forces F_i, bending moment M, and distributed forces q_i acting on a beam segment

A simple model for the drive is displayed in Fig. 1: We assume, that the driving drum has radius R_2 and rotates in clockwise direction. Furthermore, we assume, that there is no slip between the belt and the drum. Since in this configuration the tension in the upper span of the belt is larger, we restrict our attention to this segment.

Before deriving the equations for the belt, we rescale the lengths by a reference length L_0, like the distance between the centers of the drum, the (generalized) forces by the pretension P_0, and the time by $\sqrt{\varrho A L_0^2/P_0}$, such that the wave speed in the belt is scaled to unity. Assuming a Kelvin-Voigt material law and an extensible Euler-Bernoulli beam model for the belt, we obtain the differential equations for a line segment displayed in Fig. 2, (see e.g. [1])

$$x' = (1+\varepsilon)\cos\vartheta, \qquad y' = (1+\varepsilon)\sin\vartheta, \tag{1a}$$

$$\varepsilon + \delta\dot{\varepsilon} = \beta N = \beta(F_1\cos\vartheta + F_2\sin\vartheta), \qquad \gamma(\vartheta' + \delta\dot{\vartheta}') = M, \tag{1b}$$

$$M' = (1+\varepsilon)(F_1\sin\vartheta - F_2\cos\vartheta), \tag{1c}$$

$$F_1' = -q_1 + \ddot{x}, \qquad F_2' = -q_2 + \ddot{y}. \tag{1d}$$

Here $(\cdot)'$ denotes the derivative w.r.t. the rescaled unstrained arc length s, ϑ is the inclination angle, δ is the damping parameter, $\beta = P_0/EA$ is the elongation due to pre-stretching and $\gamma = EJ/(P_0 L_0^2)$ is the bending stiffness. For typical belts the parameters δ, β and γ are very small.

In (1) the arc-length s denotes the length from a certain material point of the belt. In order to study steady motions, we set $s = S + vt$, where the new variable S denotes the length along a steady configuration. With

$$\frac{\partial u(s,t)}{\partial s} = \frac{\partial u(S+vt,t)}{\partial S} \quad \text{and} \quad \frac{\partial u(s,t)}{\partial t} = \frac{\partial u(S+vt,t)}{\partial t} + \frac{\partial u(S+vt,t)}{\partial S}v$$

* Corresponding author: e-mail Alois.Steindl@tuwien.ac.at, phone +0043 1 58801 325208, fax +0043 1 58801 9325208

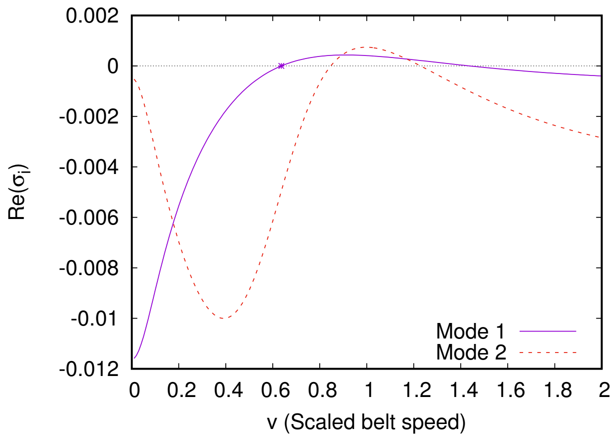

Fig. 3: Variation of the critical eigenvalues for varying belt speeds v. At $v \approx 0.64$ a Hopf bifurcation occurs.

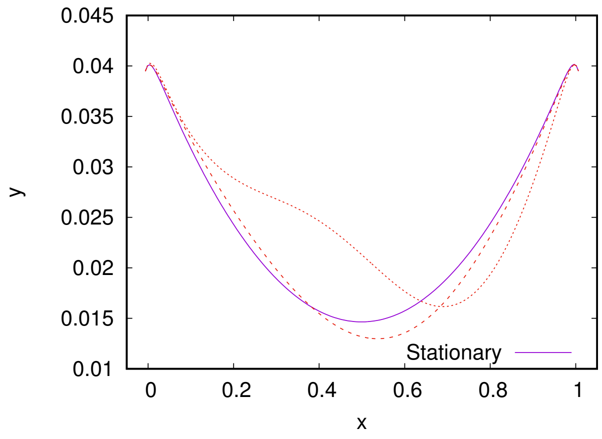

Fig. 4: Shape of the stationary state and the critical oscillations at the Hopf bifurcation point

the time derivatives $\dot{u}$ in (1) have to be replaced by $vu' + \dot{u}$, where the prime now denotes the derivative w.r.t. S. Therefore the material laws and the equilibrium equations in (1) become

$$N = \varepsilon + \delta(v\varepsilon' + \dot{\varepsilon}), \qquad M = \gamma(\vartheta' + \delta(v\vartheta'' + \dot{\vartheta}')), \tag{1b'}$$

$$F_1' = -q_1 + v^2 x'' + 2v\dot{x}' + \ddot{x}, \qquad F_2' = -q_2 + v^2 y'' + 2v\dot{y}' + \ddot{y}, \tag{1d'}$$

where x'' and y'' are obtained by differentiating (1a). Since the parameters δ and γ are usually very small, the equations (1b') are severely singularly perturbed.

The boundary conditions at the endpoints state, that the free portion of the belt starts and ends at the circumference of the drums and that the curvature is given by the radius of the drums. Further the time derivatives of ε and M vanish at the left drum and the belt length remains constant

$$x(0) = -R_1 \sin\vartheta(0), \qquad x(L) = x_1 - R_2 \sin\vartheta(L), \tag{2a}$$

$$y(0) = R_1 \cos\vartheta(0), \qquad y(L) = y_1 + R_2 \cos\vartheta(L), \tag{2b}$$

$$\vartheta'(0) = -1/R_1, \qquad \vartheta'(L) = -1/R_2, \tag{2c}$$

$$\varepsilon(0) = \beta N(0), \qquad \gamma\vartheta'(0) = M(0), \tag{2d}$$

$$-R_1\vartheta(0) + L + R_2\vartheta(L) = L_{\text{fix}}, \tag{2e}$$

where L_{fix} denotes the unstretched cable length between the tops of both drums. It is initially calculated by requiring $N(L) = 1$ for the undriven belt $v = 0$. Also the length L of the belt's free portion is an unknown quantity, which is obtained as part of the solution of the boundary value problem. Contrary to [2] we assume, that no slipping occurs between the belt and the drums.

2 Numerical Results

For the nondimensional parameter values $R_1 = R_2 = 0.04$, $\beta = \delta = 0.001$, $\gamma = 0.0001$, $q_1 = 0$, $q_2 = -0.2$ the stationary state and the eigenvalues were calculated for $v \in [0.01, 2]$ using the BVP-solver Colsys ([3]) and the continuation procedure Hom ([4]). The variation of the least stable eigenvalues over the drive speed v is displayed in Fig. 3, the shape of the stationary state of the moving belt and the critical eigenfunctions at the Hopf bifurcation point is shown in Fig. 4. The strong bending at the end points is clearly visible. While the stationary state is almost symmetrical, the eigenfunctions have a quite asymmetrical shape. For the considered range of parameter values all other eigenvalues remain stable.

References

[1] J. A. Wickert and C. D. Mote, J. Appl. Mech **57**(3), 738–744 (1990).
[2] V. Eliseev and Y. Vetyukov, Acta Mech **223**, 1657–1667 (2012).
[3] U. M. Asher, J. Christiansen, and R. D. Russell, Math. Comp **33**, 659 – 679 (1978).
[4] R. Seydel, A continuation algorithm with step control, in: Numerical methods for bifurcation problems. ISNM 70, (Birkhäuser, 1984).